



1 **Landfast ice thickness in the Canadian Arctic Archipelago from Observations and Models**

2 Stephen. E. L. Howell¹, Frédéric Laliberté¹, Ron Kwok², Chris Derksen¹ and Joshua King¹

3 ¹Climate Research Division, Environment Canada, Toronto, Canada

4 ²Jet Propulsion Laboratory, California Institute of Technology, Pasadena, California, USA

5 **Abstract**

6 Observed and modelled landfast ice thickness variability and trends spanning more than five
7 decades within the Canadian Arctic Archipelago (CAA) are summarized. The observed sites
8 (Cambridge Bay, Resolute, Eureka and Alert) represent some of the Arctic's longest records of
9 landfast ice thickness. Observed end-of-winter (maximum) trends of landfast ice thickness (1957-
10 2014) were statistically significant at Cambridge Bay (-4.31 ± 1.4 cm decade⁻¹), Eureka (-4.65 ± 1.7
11 cm decade⁻¹) and Alert (-4.44 ± 1.6 cm decade⁻¹) but not at Resolute. Over the 50+ year record, the
12 ice thinned by ~0.24-0.26 m at Cambridge Bay, Eureka and Alert with essentially negligible
13 change at Resolute. Although statistically significant warming in spring and fall was present at all
14 sites, only low correlations between temperature and maximum ice thickness were present; snow
15 depth was found to be more strongly associated with the negative ice thickness trends. Comparison
16 with multi-model simulations from Coupled Model Intercomparison project phase 5 (CMIP5),
17 Ocean Reanalysis Intercomparison (ORA-IP) and Pan-Arctic Ice-Ocean Modeling and
18 Assimilation System (PIOMAS) show that although a subset of current generation models have a
19 'reasonable' climatological representation of landfast ice thickness and distribution within the
20 CAA, trends are unrealistic and far exceed observations by up to two magnitudes. ORA-IP models
21 were found to have positive correlations between temperature and ice thickness over the CAA, a
22 feature that is inconsistent with both observations and coupled models from CMIP5.

23



24 1. Introduction

25 Landfast sea ice is immobile ice that is grounded or anchored to the coast [Barry *et al.*,
26 1979]. In the Arctic, this ice typically extends to the 20-30 m isobath. It melts each summer and
27 reforms in the fall but there are regions along the northern coast of the Canadian Arctic
28 Archipelago (CAA) where multi-year landfast ice (also termed an “ice plug”) is present. The two
29 most prominent regions of multi-year landfast sea ice in the CAA are located in Nansen Sound
30 and Sverdrup Channel [Serson, 1972; Serson, 1974] (Figure 1). It has been documented that ice
31 remained intact from 1963-1998 in Nansen Sound and from 1978-1998 in Sverdrup Channel
32 [Jeffers *et al.*, 2001; Melling, 2002; Alt *et al.*, 2006]. The extreme warm year of 1998 disintegrated
33 the ice in both regions and their survival during the summer melt season in recent years has
34 occurred less frequently [Alt *et al.*, 2006]. Over the entire Arctic, landfast ice extent is declining at
35 7% decade⁻¹ since the mid-1970s [Yu *et al.*, 2013]

36 Records of landfast ice thickness provide annual measures of ice growth that can also
37 almost entirely be attributed to atmospheric forcing with negligible deep ocean influence on local
38 ice formation. While the key forcings on landfast ice and offshore ice are different, the seasonal
39 behavior of landfast ice can nevertheless provide useful information for understanding the
40 interannual variability of ice thickness in both regimes. Presently, there is no pan-Arctic network
41 for monitoring changes in landfast ice but available measurements suggest thinning in recent years.
42 Thickness measurements near Hopen, Svalbard revealed thinning of landfast ice in the Barents
43 Sea region by 11 cm decade⁻¹ between 1966 and 2007 [Gerland *et al.*, 2008]. From a composite
44 time series of landfast ice thickness from 15 stations along the Siberian coast, Polyakov *et al.*
45 [2010] estimate an average rate of thinning of 3.3 cm decade⁻¹ between the mid-1960s and early



46 2000s. Relatively recent observations by *Mahoney et al.* [2007] and *Druckenmiller et al.* [2009]
47 found longer ice-free seasons and thinner landfast ice compared to earlier records.

48 At four sites in the CAA, *Brown and Cote* [1992] (hereinafter, BC92) provided the first
49 examination of the interannual variability of end-of-winter (maximum) landfast ice thickness and
50 associated snow depth over the period 1957-1989. Their results highlighted the insulating role of
51 snow cover in explaining 30-60% of the variance in maximum ice thickness. Similar results were
52 also reported by *Flato and Brown* [1996] and *Gough et al.* [2004]. In the record examined by
53 BC92, no evidence for systematic thinning of landfast ice in the CAA was found. Landfast ice
54 thickness records at several of these CAA sites are now over 50 years in length, which represents
55 an addition of more than two decades of measurements since BC92 during a period that saw
56 dramatic reductions in the extent and thickness of Arctic sea ice [e.g. *Kwok and Rothrock*, 2009;
57 *Stroeve et al.*, 2012].

58 The sparse network of long term observations of snow and ice thickness in the Arctic
59 (clearly exhibited by only four ongoing measurements sites operated by Environment Canada in
60 the CAA) has made the use of models imperative to provide a broader regional scale perspective
61 of sea ice trends in a warming climate. Given the coarse spatial resolution of global climate models,
62 previous studies focusing on the CAA have relied on either a one-dimensional thermodynamic
63 dynamic model [*Flato and Brown*, 1996; *Dumas et al.*, 2006] or a regional three-dimensional ice-
64 ocean coupled model [e.g. *Sou and Flato*, 2009]. Specifically, *Dumas et al.* [2006] found projected
65 maximum ice thickness decreases of 30 cm by 2041-2060 and 50 cm by 2081-2100 and *Flato and*
66 *Sou* [2009] reported a potential 17% decrease in overall ice thickness throughout the CAA by
67 2041-2060. However, in recent years some global climate models, reanalysis products, and data



68 assimilation systems are now of sufficient spatial resolution to assess potential landfast ice
69 thickness changes within the CAA.

70 This analysis examines the trends of measured landfast ice thickness, snow depth and air
71 temperature over a 50+ year period between 1957 and 2014 and compares the results with the
72 earlier analysis by BC92. We then use this observational foundation to evaluate the
73 representativeness of landfast ice in state-of-the-art global climate models, assimilation systems
74 and re-analysis products.

75

76 **2. Data Description**

77 **2.1. Observations**

78 Landfast ice thickness and corresponding snow depth measurement have been made
79 regularly at many coastal stations throughout Canada since about 1950. These data are quality
80 controlled and archived at the Canadian Ice Service (CIS) and represent one of the few available
81 sources of continuous ice thickness measurements in the Arctic. In general, thickness
82 measurements are taken once per week, starting after freeze-up when the ice is safe to walk on and
83 continuing until breakup or when the ice becomes unsafe. Complete details of this dataset are
84 provided by Brown and Cote (1992) and the dataset is available on the CIS web site
85 (<http://www.ec.gc.ca/glaces-ice/>, see Archive followed by Ice Thickness Data). Four sites in the
86 CAA were selected for study: Alert, Eureka, Resolute, and Cambridge Bay (Figure 1). Although
87 there are other sites in the database, these sites are the only ones than span the same 55-year period
88 between 1960 and 2014. The record at Mould Bay, used in BC92, terminated in the early 1990s.
89 Together these sites cover $\sim 20^\circ$ in latitude (Figure 1) that are adjacent to an area of thick Arctic
90 sea ice that experienced the highest thinning in recent years [Kwok and Rothrock, 2009; Laxon et



91 *al.*, 2013]. Values of maximum or end-of-winter ice thickness and corresponding snow depth
92 during the ice growth season were extracted from the weekly ice and snow thickness data at the
93 selected sites. As this study is concerned with annual variability in maximum ice thickness, the
94 main period of interest extends from September to late May.

95 The other source of observed data used in this study were monthly mean air temperature
96 records at Alert, Eureka, Resolute, and Cambridge Bay for which a complete description is
97 provided by *Vincent et al.* [2012].

98

99 **2.2. Models**

100 The representation of CAA landfast sea ice thickness within the Coupled Model
101 Intercomparison project phase 5 (CMIP5) is analyzed using the 1980-2005 Historical experiment
102 followed by the 2006-2099 Representative Concentration Pathway 8.5 (RCP85) experiment
103 [*Taylor et al.*, 2012] (Table 1). Monthly sea ice thickness (variable *sit*), sea ice concentration
104 (variable *sic*), 2 meter temperature (variable *tas*) and snow depth (variable *snd*) were used. The
105 CMIP5 data were retrieved from the British Atmospheric Data Centre database and accessed
106 through the Center for Environmental Data Analysis (www.ceda.ac.uk). Ensemble r6i1p1 and
107 r7i1p1 from model EC-EARTH were removed because of corrupted data. We obtain the multi-
108 model mean of trends at each grid point by creating the distribution of trends through a Monte-
109 Carlo simulation. We use a t-distribution for the interannual variability and build a noise model to
110 account for internal variability as in *Swart et al.* [2014] and *Laliberté et al.* [2016]. The multi-
111 model mean and its statistical significance is then obtained from the distribution. We obtain the
112 multi-model mean of Pearson correlations by first performing a Fisher transform and then apply



113 the same method as for the trends. The inverse Fisher transform is applied after obtaining the multi-
114 model mean and its significance.

115 We also investigate ice thickness values from a selection of the highest resolution models
116 [Storto *et al.*, 2011; Forget *et al.*, 2015; Haines *et al.*, 2014, Zuo *et al.*, 2015; Masina *et al.*, 2015]
117 from the Ocean Reanalysis Intercomparison (ORA-IP) [Balsameda *et al.*, 2015; Chevallier *et al.*,
118 2016] (Table 2) and from the Pan-Arctic Ice-Ocean Modeling and Assimilation System (PIOMAS)
119 [Zhang and Rothrock, 2003]. Supporting 2 meter temperature data was obtained from ERA-
120 Interim [Dee *et al.*, 2011].

121

122 **3. Results and Discussion: Observations**

123 **3.1. Climatology**

124 The average behavior of landfast ice at the four sites over the 50+ year record is
125 summarized in Table 3. Ice growth, approximately linear through most of the season, slows after
126 March (Figure 2). Ice thickness reaches a maximum of ~2-2.3 m by late May at all sites. Values
127 are consistent with that reported by BC92 and with recent observations of Melling *et al.* [2015]
128 and Haas and Howell [2015]. The standard deviations are nearly uniform (at ~0.2 m) across all
129 sites, giving a relatively low coefficient of variation (COV; a measure of relative dispersion
130 defined as the ratio of the standard deviation to the mean) of ~0.1. The thickest ice is found in
131 Eureka with a 1957-2014 mean of 2.27 m that is likely due to climatologically lower air
132 temperatures in the fall and winter (Table 3).

133 Snow depth also appears to grow linearly through the season, peaking in May but unlike
134 ice thickness the monthly variability is high (COV ~0.4) (Figure 3). Mean October to May snow
135 depths at Resolute, Eureka and Alert range from ~18-23 cm compared to only ~8 cm at Cambridge



136 Bay (Table 3). The rapid buildup of the snow cover due to storms in the fall and early winter that
137 is evident over the Arctic Ocean multi-year ice cover [Warren *et al.*, 1999; Webster *et al.*, 2014],
138 is not seen in these snow depth records within the CAA. The linear behavior in snow depth is likely
139 maintained by continuous wind-driven redistribution and densification throughout the ice growth
140 season [BC92; Woo and Heron, 1989].

141

142 **3.2. Trends**

143 The time series of maximum ice thickness at Cambridge Bay, Resolute, Eureka and Alert
144 are illustrated in Figure 4 and summarized in Table 1. Statistically significant (95% or greater
145 confidence level) negative maximum ice thickness trends are present at Cambridge Bay (-4.31 ± 1.4
146 cm decade^{-1}), Eureka ($-4.65 \pm 1.7 \text{ cm decade}^{-1}$) and Alert ($-4.44 \pm 1.6 \text{ cm decade}^{-1}$) (Table 1). A slight
147 negative trend is present at Resolute but not statistically significant at the 95% confidence level
148 (Table 1). Over the 50+ year record, the ice thinned by $\sim 0.24\text{--}0.26 \text{ m}$ at Cambridge Bay, Eureka
149 and Alert with essentially negligible change at Resolute. These trends in the CAA are similar to
150 trends on the Siberian coast ($-3.3 \text{ cm decade}^{-1}$) [Polyakov *et al.*, 2010] but lower in magnitude
151 compared to the Barents Sea ($-11 \text{ cm decade}^{-1}$) [Gerland *et al.*, 2008].

152 For the shorter record (late 1950s–1989, ~ 30 years) investigated by BC92 there was a
153 negative trend at Alert ($-7.1 \text{ cm decade}^{-1}$), no evidence of a trend at Eureka, and a positive trend at
154 Resolute ($10 \text{ cm decade}^{-1}$) but only the positive trend at Resolute was statistically significant at the
155 95% or greater confidence level. Our results from the present 50+ year record suggest that the
156 negative trend at Alert is robust and the trend at Eureka is now negative and significant. The trend
157 at Resolute is now slightly negative however it is not statistically significant.



158 Typically, ice thickness reaches its maximum in late May with trends toward earlier dates
159 of maximum ice thickness present at all sites (significant at Resolute, Eureka and Alert; Table 3).
160 The significant trends are between -2.0 ± 0.1 days decade⁻¹ at Eureka to -6.2 ± 1.5 days decade⁻¹ at
161 Resolute. At Resolute, the date of maximum ice thickness is now on average more than a month
162 earlier than the early 1960's suggesting a shortened growth season although this is not reflected in
163 the trend in ice thickness. Together, the trends of ice thickness and their recorded dates suggest a
164 systematic thinning of landfast ice at Cambridge Bay, Eureka and Alert.

165

166 **3.3. Ice thickness linkages with snow depth and temperature**

167 The variability of landfast thickness at these Arctic sites was previously found to be largely
168 driven by interannual variations in snow depth and air temperature [BC92; *Flato and Brown*,
169 1996]. With the 50+ year record at the four sites, we can examine the corresponding linkages to
170 snow depth and temperature which are also summarized in Table 3.

171 For snow depth, there are positive trends at Eureka and Alert and negative trends at
172 Cambridge Bay and Resolute (Figure 5). The only trend that is statistically significant at the 95%
173 confidence is Cambridge Bay at -0.8 ± 0.4 cm decade⁻¹ (Table 3). In contrast, BC92 found a
174 significant positive trend at Alert (4 cm decade⁻¹), a trend of low significance in Eureka, and a
175 negative and significant trend at Resolute (-3.3 cm decade⁻¹). Looking at the detrended correlations
176 (r) between snow depth and ice thickness reveals the strongest correlation at Resolute ($r=-0.71$)
177 followed by Eureka ($r=-0.66$), Alert ($r=-0.47$) and Cambridge Bay ($r=-0.31$). While Figure 6
178 provides evidence from extreme years of the role of deeper snow inhibiting ice growth compared
179 to thinner snow, the expected statistical correspondence between negative trends in ice thickness
180 with positive trends in snow depth is only present at Eureka and Alert. This may in part be due to



181 the single pointwise snow depth and ice thickness measurements made at each point in time, which
182 fail to capture spatial heterogeneity in the snow depth/ice thickness relationship.

183 With respect to observed temperature, we find significant warming trends in the spring and
184 fall at all sites over the 50+ year record (Table 3; Figure 7). Significant warming is also present at
185 all sites in the summer except Resolute and at all sites during the winter except Eureka (Table 3).
186 Warming is highest during the fall, at $\sim 0.6^{\circ}\text{C decade}^{-1}$ at all sites (Table 3). The linkage between
187 temperature and maximum ice thickness weaker than compared to snow depth as only at the
188 Cambridge Bay site is warming in the spring and winter associated with decreases in maximum
189 ice thickness with a detrended correlation of ~ 0.4 . This may indicate that temperature plays more
190 of a role at influencing maximum ice thickness at Cambridge Bay as this site also experienced the
191 lowest detrended correlation with snow depth ($r=-0.31$).

192 Also of interest is that the observed temperature trends over this period differ considerably
193 than the earlier period investigated in BC92, in which they reported cooling at all the sites, with a
194 significant cooling trend at Eureka. It was noted that the general cooling over their record coincided
195 with the 1946-1986 cooling trend over much of the eastern Arctic and northwest Atlantic reported
196 by *Jones et al.* [1987]. This cooling trend halted during the 1980s and the warming, seen in the
197 current and longer record, has resumed [*Jones et al.*, 1999]. Arctic land areas have experienced an
198 overall warming of about $\sim 2^{\circ}\text{C}$ since the mid-1960s, with area-wide positive temperature
199 anomalies that show systematic changes since the end of the 20th century, which continued
200 through 2014 [*Jeffries and Richter-Menge*, 2015]. Recently, warming in Canadian Arctic regions
201 was found to be greater than the pan-Arctic trend by up to $0.2^{\circ}\text{C decade}^{-1}$ [*Tivy et al.*, 2011].

202

203 **4. Results and Discussion: Models**



204 4.1. Climatology

205 In order to compare seasonal cycles and trends in landfast ice thickness and snow depth
206 between models and observations, we limit our comparison to models with a reasonable
207 representation of the CAA, i.e. those with an open Parry Channel (i.e. bcc-csm-1-1, bcc-csm-1-
208 1m, CNRM-CM5, ACCESS1-0, ACCESS1-3, FIO-ESM, EC-EARTH, inmcm4, MIROC5, MPI-
209 ESM-LR, MPI-ESM-MR, MRI-CGCM3, CCSM4, NorESM1-M, NorESM1-ME, GFDL-CM3,
210 GFDL-ESM2G, GFL-ESM2M, CESM1-BCG, CESM1-CAM5, CESM-WACCM). In these
211 models, sufficient spatial resolution allows us to find sample points that are almost collocated to
212 *in situ* observation locations. The sample points were determined by finding the closest ocean grid
213 point where the sea ice is packed for a good portion of year but not all year. Grid points with this
214 characteristic therefore share the most important feature of the landfast ice at our observations
215 locations: it is not perennial. Mathematically, we sought sample points where the sea ice
216 concentration is on average above 85% for more than one month but less than 11 months over the
217 1955-2014 period. The Eureka site is however particularly challenging for models because it lies
218 deep in a very narrow channel, which is only resolved by the MPI-ESM-MR in the CMIP5. As a
219 result, for most models, the sample point for Eureka is located on the western shore of Ellesmere
220 Island.

221 The seasonal cycle (1955-2014) of median ice thickness from CMIP5 (black), ORA-IP
222 models CGLORS, ORAP5.0 and GLORYS2V3 (blue), ECCO-v4 (green) and UR025.4 (red) is
223 shown in Figure 8. ORA-IP models have been split into three groups based, respectively, on their
224 high, medium and low ice thicknesses at Alert. Ice thickness from CMIP5 is comparable to
225 observations (Figure 2) at Cambridge Bay and Resolute with maximum ice thickness reaching 200
226 cm. The ORA-IP models are less consistent. ECCO-v4 tends to have thicker sea ice than



227 observations at Cambridge Bay, Resolute and Eureka but thinner at Alert. CGLORS, ORAP5.0,
228 and GLORYS2V3, on the other hand, are comparable to observations at Cambridge Bay, Resolute
229 and Eureka but have extremely thick and perennial ice close to Alert.

230 The seasonal cycle (1955-2014) of median snow depth from CMIP5 is shown in Figure 9.
231 CMIP5 models indicate a linear increase similar to observations reaching a maximum of ~20 cm
232 in April or May. This is lower than the observed maximum at Resolute, Eureka and Alert but is
233 about twice as much as at Cambridge Bay. While the snow depth reaches zero during the summer
234 at Eureka and Alert in models, the sea ice thickness does not (Figure 8), unlike in observations.
235 This likely reflects the fact that thick, mobile ice is located in the vicinity of these sample points
236 in models. The seasonal cycle over packed ice in these models thus gives a reasonable
237 representation of the seasonal cycle over landfast ice in the CAA, especially in the southern region
238 of the CAA. Overall, this comparison shows how recent improvements in sea ice model resolution
239 allows comparisons with observations that required dynamical downscaling techniques in the
240 previous generation of sea ice models [i.e. *Dumas et al. 2005; Sou and Flato, 2013*].

241 Despite relatively high spatial resolution, PIOMAS does not resolve seasonal ice thickness
242 along the coasts and within the very narrow channels within the CAA (not shown). As a result,
243 Cambridge Bay and Resolute Bay sites represent the only long-term monitoring sites within the
244 CAA suitable for comparison since PIOMAS. The monthly time series of PIOMAS ice and snow
245 thickness estimates at Cambridge Bay and Resolute is shown in Figure 10. The seasonal cycle of
246 ice growth at Cambridge Bay and Resolute is representative compared to observations (Figure 2)
247 but PIOMAS estimates retain more ice in August and September, particularly at Resolute. Ice
248 growth reaches a maximum in April at Cambridge and in May at Resolute which is 1-month earlier
249 compared to observations. Snow depth follows a linear increase similar to observations (Figure 3)



250 with good agreement at Cambridge Bay but considerably underestimates snow depth at Resolute
251 (Figure 10). *Schweiger et al.* [2011] performed a detailed comparison of PIOMAS ice thickness
252 values against *in situ* and Ice, Cloud, and land Elevation Satellite (ICESat) ice thickness
253 observations and found strong correlations. They determined a root mean square error (RMSE) of
254 ~0.76 m and noted that PIOMAS generally overestimates thinner ice and underestimates thicker
255 ice. At both sites within the CAA, PIOMAS ice thickness data is in reasonably good agreement
256 with *in situ* observations with RMSE's of 0.29 cm at Cambridge Bay and 0.68 cm at Resolute
257 (Figure 11). The systematic overestimate of thinner ice reported by *Schweiger et al.* [2011] is more
258 apparent at Resolute than Cambridge Bay (Figure 11). The higher latitude regions of the CAA
259 where there is an intricate mix of seasonal first-year ice and multi-year ice is a problem for
260 PIOMAS and thus contributes to the larger discrepancy at Resolute compared to Cambridge Bay.
261

262 **4.2. Trends**

263 The spatial distribution of maximum sea ice thickness trends from ORA-IP and CMIP5 is
264 illustrated in Figures 12. It is particularly apparent that the high resolution models exhibit a similar
265 North-South trend pattern as for the observational stations (Figure 2), albeit with overestimated
266 negative thickness trends. The general pattern and magnitude of the thickness trends are roughly
267 in accordance with the temperature trends in these models (not shown). One exception is the ORA-
268 IP CGLORS that have positive thickness trends (Figure 12a). This is robust and it appears that the
269 model is not completely equilibrated in the CAA and exhibit large month-to-month adjustments.
270 Model ORAP5.0 also is not completely equilibrated in the region for years 1979-1984. During
271 those years, it exhibits large inter annual changes in thickness. For this reason, we are only
272 considering years 1985-2013 for this model.



273 For PIOMAS, the North-South overestimated trend is also present (not shown) as with
274 CMIP5 and ORA-IP. Looking specifically at trends near the observed sites indicates that the mean
275 maximum ice thickness linear trend from at Cambridge Bay is -13.4 ± 3.4 cm decade⁻¹ which is
276 almost double the observational trend of 6.2 ± 2.4 cm decade⁻¹. At Resolute, the PIOMAS linear
277 trend is 24.0 ± 4.1 cm decade⁻¹ which is considerably stronger than the observational trend of -
278 4.9 ± 3.51 cm decade⁻¹.

279

280 **4.3. Ice thickness linkages with snow depth and temperature**

281 Even though ORA-IP models have unrealistically large thickness trends, the pattern of inter
282 annual correlation (detrended) between winter temperatures and thicknesses is roughly consistent
283 across models (Figure 13). Some ORA-IP models also experience positive correlations (e.g.
284 CGLORS, ORAP5.0, GLORYS2V3 and UR025.4) that are mostly located north of the CAA or
285 within the CAA in regions where multi-year ice is known to be present. It is possible that warmer
286 temperatures are associated with an increased flux of thicker multi-year ice into the CAA which is
287 known to occur [e.g. *Howell et al.*, 2013] but the driving processes responsible for these positive
288 correlations require more investigation. In CMIP5 models, no model exhibits positive correlations
289 with temperature that resemble ORA-IP models over the CAA. Although the time series for the
290 ORA-IP models is short and the positive correlations are not statistically significant, this behavior
291 suggest that care should be taken when using these ORA-IP models to study the interannual
292 variability in the Canadian Arctic.

293 In the CMIP5 models, significant winter snow depth trends are more strongly negative in
294 the North than in the South (Figure 14). This is in disagreement with point observations presented
295 in the previous sections that showed slightly positive snow depth trends at Alert and negative



296 trends at Cambridge Bay. Although only based on limited point *in situ* observations, this suggests
297 that over the last decades winter precipitation at Alert increased faster than warming temperature
298 could increase melting, a compensation that is clearly not captured in CMIP5 models.

299

300 **5. Conclusions**

301 Over the 50+ year *in situ* observational record, negative trends in maximum (end-of-winter)
302 ice thickness are found at all four sites with statistically significant trends present at Cambridge
303 Bay, Eureka and Alert. Negative trends in the day of maximum ice thickness are also present at all
304 sites and statistically significant at Resolute, Eureka and Alert. Together, these trends suggest
305 thinning of landfast ice in the CAA, where little evidence was found in the shorter record analyzed
306 in an earlier study (BC92). Even though warming is seen at all sites, changes in ice thickness is
307 also attributable to variability in snow depth, which plays a dominant role in controlling the
308 interannual mean and variability of ice thickness. Within the CAA, increases in snow depth are
309 contributing to decreased trends in maximum ice thickness at Eureka and Alert but thus far appear
310 to be exerting less of an impact on maximum ice thickness at Resolute and Cambridge Bay. Freeze
311 onset at these sites is increasing at $\sim 3\text{-}6$ days decade⁻¹ [Howell *et al.*, 2009] and the delayed ice
312 formation could play more of a role at the in the southern sites because of a longer open water
313 season.

314 Comparison of CMIP5, ORA-IP and PIOMAS simulations with observations indicate a
315 reasonable representation of the landfast ice thickness monthly climatology within the CAA. This
316 is particularly apparent when seasonal first-year ice dominates the icescape (i.e. Cambridge Bay).
317 Despite improvements in spatial resolution, mixed ice types (i.e. seasonal and multi-year) present
318 at the sub-grid cell resolution are likely problems for model estimates within the CAA. The overall



319 thickness of ice within the CAA in the current generation of models is too high. As a result, trends
320 are unrealistic and far exceed observations (by upwards of $-50 \text{ cm decade}^{-1}$) in part because the
321 initial ice thickness is too large. The problem is particularly acute in the ORA-IP models where
322 large and unrealistic inter annual changes in thickness suggest that the models are not fully
323 equilibrated.

324 Over the mobile Arctic Ocean ice cover, the combined record of submarine and ICESat
325 thickness estimates suggest that winter sea ice thickness in the central Arctic has thinned from 3.64
326 m in 1980 to 1.75 m by 2009 [Rothrock *et al.*, 2008; Kwok and Rothrock, 2009] – a linear rate of
327 over $-60 \text{ cm decade}^{-1}$ that is mostly due to the loss of multi-year ice. However, the contribution of
328 seasonal ice to that rate is not available. As seasonal ice, becomes the dominant ice type, the focus
329 has shifted to understanding the behavior of seasonal ice thickness. Between 1991 and 2003,
330 Melling *et al.* [2005] found only a small trend ($-7 \text{ cm decade}^{-1}$), though of low statistical
331 significance, in the seasonal pack in the Beaufort Sea. In the short ICESat record of ice thickness
332 (2003-2008), Kwok *et al.* [2009] also found negligible trend in the seasonal ice cover. This led
333 them to speculate that a thinner snow cover during to the later start of the growth season is
334 conducive to higher ice production as a result of reduced accumulation of that large fraction of
335 snow that typically falls in October and November. However, over the seasonal ice cover there is
336 the additional contribution of ice deformation on the mean of the thickness distribution.

337 While the impact of the snow cover on ice thickness is well known, the significant
338 correlations at Resolute, Eureka and Alert suggest that the higher sensitivity to changes in snow
339 depth could easily mask the warming signal on both fast and offshore ice. The dependency between
340 ice thickness trends and warming trends is only weakly present at Cambridge Bay ($r=0.4$) and
341 further points out the dominance of snow depth because of the large variability of the thickness



342 trends compared to the relatively low scatter in the temperature trends. Thus, even in this limited
343 data set, we can see the dominant role played by snow depth in determining the interannual
344 variability of the maximum landfast ice thickness. This again highlights that the primary factor is
345 the amount and timing of snow accumulation, not air temperature. However, it is worth noting that
346 few of the current generation models show coherent relationships between ice thickness, snow
347 depth and temperature over the longer term record.

348

349 **Authors Contributions**

350 S.E.L.H, F.L and R.K designed the study, performed the analysis and wrote the manuscript with
351 input from C.D. and J.K.

352

353 **Acknowledgements**

354 The authors wish to thank all the individuals responsible for collecting landfast ice and snow
355 thickness measurements in the Canadian Arctic over the past 50+ years.

356

357

358 **References**

359

360 Alt, B., K. Wilson, and T. Carrieres (2006), A case study of old ice import and export through
361 Peary and Sverdrup channels in the Canadian Arctic Archipelago: 1998-2004, *Ann. Glaciol.*, 44,
362 329–338, doi:10.3189/172756406781811321.

363

364 Barry, R. G., R. E. Moritz, and J. C. Rogers (1979), The fast ice regimes of the Beaufort and
365 Chukchi sea coasts, Alaska, *Cold Reg. Sci. Technol.*, 1, 129– 152.

366

367 M.A. Balmaseda , F. Hernandez , A. Storto , M.D. Palmer , O. Alves , L. Shi , G.C. Smith , T.
368 Toyoda , M. Valdivieso , B. Barnier , D. Behringer , T. Boyer , Y-S. Chang , G.A. Chepurin , N.
369 Ferry , G. Forget , Y. Fujii , S. Good , S. Guinehut , K. Haines , Y. Ishikawa , S. Keeley , A.
370 Köhl , T. Lee , M.J. Martin , S. Masina , S. Masuda , B. Meyssignac , K. Mogensen , L. Parent ,
371 K.A. Peterson , Y.M. Tang , Y. Yin , G. Vernieres , X. Wang , J. Waters , R. Wedd , O. Wang ,
372 Y. Xue , M. Chevallier , J-F. Lemieux , F. Dupont , T. Kuragano , M. Kamachi , T. Awaji , A.
373 Caltabiano , K. Wilmer-Becker , F. Gaillard, The Ocean Reanalyses Intercomparison Project



- 374 (ORA-IP), *Journal of Operational Oceanography*, Vol. 8, Iss. sup1, 2015,
375 DOI:10.1080/1755876X.2015.1022329
376
377 Brown, R., and P. Cote (1992), Interannual variability of landfast ice thickness in the Canadian
378 high arctic, 1950–89. *Arctic*, 45, 273–284.
379
380 Bromwich, D. H., A. B. Wilson, L. Bai, G. W. K. Moore, and P. Bauer, 2015: A comparison of
381 the regional Arctic System Reanalysis and the global ERA-Interim Reanalysis for the Arctic. *Q.*
382 *J. R. Meteorol. Soc.*, doi: 10.1002/qj.2527
383
384 Dee DP, co-authors (2011), The ERA-Interim reanalysis: configuration and performance of the
385 data assimilation system. *Q J R Meteorol Soc.* 137: 553–597, doi:10.1002/qj.828.
386
387 Dumas, J. A., G. M. Flato, and R. D. Brown (2006), Future projections of landfast ice thickness
388 and duration in the Canadian Arctic. *J. Climate*, 19, 5175–5189.
389
390 Druckenmiller, M. L., H. Eicken, M. A. Johnson, D. J. Pringle, and C. C. Williams (2009),
391 Toward an integrated coastal sea-ice observatory: System components and a case study at
392 Barrow, Alaska. *Cold Reg.Sci.Tech.*, 56, 61-72.
393
394 Flato, G. M., and R. D. Brown (1996), Variability and climate sensitivity of landfast Arctic sea
395 ice. *J. Geophys. Res.*, 101 (C10), 25 767–25 777.
396
397 Forget, G., Campin, J.-M., Heimbach, P., Hill, C. N., Ponte, R. M., and Wunsch, C. (2015),
398 ECCO version 4: an integrated framework for non-linear inverse modeling and global ocean
399 state estimation, *Geosci. Model Dev.*, 8, 3071-3104, doi:10.5194/gmd-8-3071-2015/
400
401 Gerland, S., A. H. H. Renner, F. Godtlielsen, D. Divine, and T. B. Loynning (2008), Decrease of
402 sea ice thickness at Hopen, Barents Sea, during 1966-2007. *Geophys. Res. Lett.*, 35, L06501.
403
404 Gough, W., A.S. Gagnon and H.P Lau (2004), Interannual variability of Hudson Bay Ice
405 Thickness, *Polar Geography*, 28(3), 222-238.
406
407 Haines K, M. Valdivieso, H. Zuo, and V.N. Stepanov (2012), Transports and budgets in a 1/4 °
408 global ocean reanalysis 1989–2010. *Ocean Sci.* 8(3): 333–344, doi:10.5194/os-8-333-
409 2012.002/qj.2063.
410
411 Haas, C., and S. E. L. Howell (2015), Ice thickness in the Northwest Passage, *Geophys. Res.*
412 *Lett.*, 42, doi:10.1002/2015GL065704
413
414 Howell, S. E. L., C. R. Duguay, and T. Markus (2009), Sea ice conditions and melt season
415 duration variability within the Canadian Arctic Archipelago: 1979–2008, *Geophys. Res. Lett.*,
416 36, L10502, doi:10.1029/2009GL037681.
417
418 Howell, S. E. L., T. Wohleben, M. Daboor, C. Derksen, A. Komarov, and L. Pizzolato (2013),
419 Recent changes in the exchange of sea ice between the Arctic Ocean and the Canadian Arctic
Archipelago, *J. Geophys. Res. Oceans*, 118, 3595–3607, doi:10.1002/jgrc.20265.



- 420 Jeffers, S., T. Agnew, B. Alt, R. De Abreu, and S. McCourt (2001), Investigating the anomalous
421 sea ice conditions in the Canadian High Arctic (Queen Elizabeth Islands) during the summer of
422 1998, *Ann. Glaciol.*, 33, 507– 612.
423
- 424 Jeffries, M. O. and J. Richter-Menge, Eds. (2015), The Arctic [in State of the Climate in 2014],
425 *Bull. Amer. Meteor. Soc.*, 96, ES1–ES32.
426 doi: <http://dx.doi.org/10.1175/2015BAMSStateoftheClimate.1>
427
- 428 Jones, P.D., T.M.L. Wigley, C.K. Folland and D.E. Parker (1987), Spatial patterns in recent
429 worldwide temperature trends. *Climate Monitor*, 16(5): 175-185.
430
- 431 Jones, P.D., M. New, D.E. Parker, S. Martin, and I.G. Rigor (1999), Surface air temperature and
432 its changes over the past 150 years, *Rev. Geophys*, 37(2),173–200.
433
- 434 Kwok, R., and D. A. Rothrock (2009), Decline in Arctic sea ice thickness from submarine and
435 ICESat records: 1958 – 2008, *Geophys. Res. Lett.*, 36, L15501, doi:10.1029/2009GL039035.
436
- 437 Kwok, R., G. F. Cunningham, M. Wensnahan, I. Rigor, H. J. Zwally, and D. Yi (2009), Thinning
438 and volume loss of Arctic sea ice: 2003-2008, *J. Geophys. Res.*, doi:10.1029/2009JC005312.
439
- 440 Laliberté, F., S. E. L. Howell, and P. J. Kushner (2016), Regional variability of a projected sea
441 ice-free Arctic during the summer months, *Geophys. Res. Lett.*, 43, 256–263,
442 doi:10.1002/2015GL066855.
443
- 444 Laxon S. W., K. A. Giles, A. L. Ridout, D. J. Wingham, R. Willatt, R. Cullen, R. Kwok, A.
445 Schweiger, J. Zhang, C. Haas, S. Hendricks, R. Krishfield, N. Kurtz, S. Farrell and M. Davidson
446 (2013), CryoSat-2 estimates of Arctic sea ice thickness and volume, *Geophys. Res. Lett.*, 40,
447 732–737, doi:10.1002/grl.50193.
448
- 449 Masina, S. et al. (2015), An ensemble of eddy-permitting global ocean reanalyses from the
450 MyOcean project. *Clim. Dynam.* 1–29, doi:10.1007/s00382-015-2728-5
451
- 452 Mahoney, A., H. Eicken, and L. Shapiro (2007), How fast is landfast sea ice? A study of the
453 attachment and detachment of nearshore ice at Barrow, Alaska. *Cold Reg.Sci.Tech.*, 47, 233-255.
454
- 455 Melling, H. (2002), Sea ice of the northern Canadian Arctic Archipelago, *J. Geophys. Res.*,
456 107(C11), 3181, doi:10.1029/2001JC001102.
457
- 458 Melling, H., D. A. Riedel, and Z. Gedalof (2005), Trends in the draft and extent of seasonal pack
459 ice, Canadian Beaufort Sea, *Geophys. Res. Lett.*, 32, L24501, doi:10.1029/s2005GL024483.
460
- 461 Melling, H., C. Haas, and E. Brossier (2015), Invisible polynyas: Modulation of fast ice
462 thickness by ocean heat flux on the Canadian polar shelf, *J. Geophys. Res. Oceans*, 120, 777–
463 795, doi:10.1002/2014JC010404.
- 464 Ólason, E. Ö. (2012), Dynamical modeling of Kara Sea land-fast ice, PhD thesis, Univ. of
465 Hamburg, Hamburg, Germany.



- 466 Polyakov, I. V., et al. (2010), Arctic Ocean Warming Contributes to Reduced Polar Ice Cap.
467 *Journal of Physical Oceanography*, 40, 2743-2756
468
- 469 Schweiger, A., R. Lindsay, J. Zhang, M. Steele, H. Stern, and R. Kwok (2011), Uncertainty in
470 modeled Arctic sea ice volume, *J. Geophys. Res.*, 116, C00D06, doi:10.1029/2011JC007084.
471
- 472 Serson, H.V. (1972), Investigations of a plug of multiyear old sea ice in the mouth of Nansen
473 Sound. Ottawa, Ont., Department of National Defence, Canada. Defence Research Establishment
474 Ottawa. (DREO Tech. Note 72-6.)
475
- 476 Serson, H.V. (1974), Sverdrup Channel. Ottawa, Ont., Department of National Defence, Canada.
477 Defence Research Establishment Ottawa. (DREO Tech. Note 74-10.)
478
- 479 Sou, T., and G. Flato (2009), Sea ice in the Canadian Arctic Archipelago: Modeling the past
480 (1950-2004) and the future (2041-60), *J. Clim.*, 22, 2181–2198, doi:10.1175/2008JCLI2335.1
481 Stroeve, J. C., M. C. Serreze, M. M. Holland, J. E. Kay, J. Malanik, and A. P. Barrett (2011),
482 The Arctic's rapidly shrinking sea ice cover: A research synthesis, *Clim. Change*, 110(3-4),
483 1005–1027.
484
- 485 Storto A, S. Dobricic S, S. Masina and D. Di Pietro (2011), Assimilating along-track altimetric
486 observations through local hydrostatic adjustments in a global ocean reanalysis system. *Mon*
487 *Wea Rev.* 139: 738–754.
488
- 489 Stroeve, J. C., M. C. Serreze, M. M. Holland, J. E. Kay, J. Maslanik, and A. P. Barrett (2012),
490 The Arctic's rapidly shrinking sea ice cover: A research synthesis, *Clim. Change*, 110(3–4),
491 1005–1027
- 492 Swart, N. C., J. C. Fyfe, E. Hawkins, J. E. Kay, and A. Jahn (2015), Influence of internal
493 variability on Arctic sea-ice trends, *Nat. Clim. Change*, 5, 86–89, doi:10.1038/nclimate2483.
494
- 495 Taylor, K. E., R. J. Stouffer, and G. A. Meehl (2012), An overview of CMIP5 and the
496 experiment design, *Bull. Am. Meteorol. Soc.*, 93, 485–498, doi:10.1175/BAMS-D-11-00094.1.
497
- 498 Tivy, A., S. E. L. Howell, B. Alt, S. McCourt, R. Chagnon, G. Crocker, T. Carrieres, and J. J.
499 Yackel (2011), Trends and variability in summer sea ice cover in the Canadian Arctic based on
500 the Canadian Ice Service Digital Archive, 1960–2008 and 1968–2008, *J. Geophys. Res.*, 116,
501 C03007, doi:10.1029/2009JC005855.
502
- 503 Vincent, L., X. Wang, E. Milewska, Hui Wan, F. Yang, and V. Swail (2012), A second
504 generation of homogenized Canadian monthly surface air temperature for climate trend analysis.
505 *Journal of Geophysical Research*, D18110, doi:10.1029/2012JD017859
506
- 507 Warren, S. G., I. G. Rigor, N. Untersteiner, V. F. Radionov, N. N. Bryazgin, Y. I. Aleksandrov,
508 and R. Colony (1999), Snow depth on Arctic sea ice, *J. Clim.*, 12, 1814–1829.
509
- 510 Wilks, D. S. (2006). On “field significance” and the false discovery rate. *J. Appl. Meteor.*
511 *Climatol.*, 45, 1181–1189. doi: <http://dx.doi.org/10.1175/JAM2404.1>



512 Woo, M-K., and R. Heron (1989), Freeze-up and break-up of ice cover on small arctic lakes. In:
513 Mackay, W.C., ed. Northern lakes and rivers. Edmonton: Boreal Institute for Northern Studies,
514 56-62.
515
516 Woo, M-K., R. Heron, P. Marsh, and P. Steer, (1983), Comparison of weather station snowfall
517 with winter snow accumulation in High Arctic basins, *Atmos.-Ocean*, 21(3):312-325.
518
519 Yu, Y, H. Stern, C. Fowler, F. Fetterer, and J. Maslanik (2014), Interannual Variability of Arctic
520 Landfast Ice between 1976 and 2007. *J. Climate*, **27**, 227–243.
521 doi: <http://dx.doi.org/10.1175/JCLI-D-13-00178.1>
522
523 Zhang, J.L. and D.A. Rothrock, (2003), Modeling global sea ice with a thickness and enthalpy
524 distribution model in generalized curvilinear coordinates, *Mon. Weather Rev.*, 131, 845-861.
525 Zuo, H., M.A. Balmaseda, and K. Mogensen (2015), The new eddy-permitting ORAP5 ocean
526 reanalysis: description, evaluation and uncertainties in climate signals. *Clim. Dynam.* 1–21.
527 doi:10.1007/s00382-015-2675-1.
528
529
530
531
532
533
534
535
536
537
538
539
540
541
542
543
544
545
546
547
548
549
550
551
552
553
554
555
556
557



558 Table 1. CMIP5 models used in this study, the number of realizations with ice data and the
 559 number of realizations with sea ice transport data

	w/ ice		w/ ice
bcc-csm1-1	1	MIROC-ESM-CHEM	1
bcc-csm1-1-m	1	MIROC5	3
BNU-ESM	1	HadGEM2-CC	1
CanESM2	5	HadGEM2-ES	4
CMCC-CESM	1	MPI-ESM-LR	3
CMCC-CM	1	MPI-ESM-MR	1
CMCC-CMS	1	MRI-CGCM3	1
CNRM-CM5	5	CCSM4	6
ACCESS1.0	1	NorESM1-M	1
ACCESS1.3	1	NorESM1-ME	1
CSIRO-Mk3.6.0	10	GFDL-CM3	1
FIO-ESM	1	GFDL-ESM2G	1
EC-EARTH	6	GFDL-ESM2M	1
inmcm4	1	CESM1(BGC)	1
FGOALS-g2	1	CESM1(CAM5)	3
MIROC-ESM	1	CESM1(WACCM)	3

560
 561
 562
 563
 564
 565
 566
 567
 568
 569
 570
 571
 572
 573
 574
 575
 576
 577
 578



579 Table 2. Summary of ORA-IP models characteristics

Model Name	CGLORS	ECCO-v4	GLORYS2V3	ORAP5.0	UR025.4
Institute	CMCC	JPL-NASA- MIT-AER	Mercator Océan	ECMWF	University of Reading
Resolution	ORCA0.25°	~40km in the Arctic	ORCA0.25°	ORCA0.25°	ORCA0.25°
Ocean Model	NEMO 3.2.1	MITgcm	NEMO 3.1	NEMO3.4	NEMO 3.2
Sea ice Model	LIM2	MITgcm	LIM2 (with EVP rheology)	LIM2	LIM2
Time period considered	1982-2012	1991-2011	1993-2013	1985-2013	1993-2010
Atmospheric forcing	ERA-Interim	ERA-Interim	ERA-Interim	ERA-Interim	ERA-Interim
Sea ice product assimilated	NSIDC NASA-Team Daily	NSIDC Bootstrap Monthly	IFREMER/CER SAT	NOAA / OSTIA combination	EUMETSAT OSI-SAF

580
 581
 582
 583
 584
 585
 586
 587
 588
 589
 590
 591
 592
 593
 594
 595
 596
 597
 598
 599
 600
 601
 602
 603
 604
 605



606 Table 3. Observed maximum ice thickness, snow depth, and surface air temperature at four
 607 landfast ice sites in the Canadian Arctic Archipelago. The bold text indicates statistical
 608 significance of the linear trend at 95% or greater.

	Cambridge Bay	Resolute	Eureka	Alert
Period	1960-2014	1957-2014	1957-2014	1957-2014
Ice Thickness, h_{ice}				
Mean of $max h_{ice}$ (m)	2.11±0.19	2.02±0.19	2.27±0.23	1.98±0.22
Trend of $max h_{ice}$ (cm decade ⁻¹)	-4.31±1.4	-0.5±1.6	-4.65±1.7	-4.44±1.6
Day of $max h_{ice}$	24 May±17	25 May±21	26 May±12	27 May±16
Trend of day of $max h_{ice}$ (days decade ⁻¹)	-0.87±1.5	-6.2±1.5	-2.0±0.1	-3.0±1.2
Snow depth (h_{snow})				
Mean Oct-May h_{snow} (cm)	8.4±4.2	22.6±10	17.6±5.8	18.4±6.2
Trend of Oct-May h_{snow} (cm decade ⁻¹)	-0.8±0.4	-0.75±0.8	0.54±0.5	0.26±0.5
Temperature				
Winter (Dec-Feb) Mean (°C)	-31.3±2.0	-30.8±1.9	-36.0±2.0	-31.2±1.6
Winter (Dec-Feb) (°C/decade)	0.59±0.2	0.35±0.1	0.23±0.2	0.38±0.1
Spring (Mar-May) Mean (°C)	-20.0±1.8	-21.1±1.8	-24.9±2.0	-22.8±1.8
Spring (Mar-May) (°C/decade)	0.47±0.1	0.57±0.1	0.44±0.1	0.32±0.1
Summer (Jun-Aug) Mean (°C)	5.9±1.4	2.3±1.3	3.9±1.2	1.3±0.8
Summer (Jun-Aug) (°C/decade)	0.30±0.1	0.17±0.2	0.21±0.1	0.1±0.1
Fall (Sep-Nov) Mean (°C)	-11.1±2.0	-13.8±2.0	-19.6±2.2	-18.0±1.7
Fall (Sep-Nov) (°C/decade)	0.60±0.2	0.67±0.1	0.68±0.2	0.56±0.1

609
 610
 611
 612
 613
 614



615 **List of Figures**

616

617 Figure 1. Map of the central Canadian Arctic Archipelago showing the location of the landfast
618 snow and thickness observations.

619

620 Figure 2. Seasonal cycle of observed mean ice thickness at the four sites (1960-2014).

621

622 Figure 3. Seasonal cycle of observed mean snow depth at the four sites (1960-2014).

623

624 Figure 4. Time series and trend of observed maximum ice thickness at the four sites.

625

626 Figure 5. Time series and trend of observed mean October through May snow depth at the four
627 sites.

628

629 Figure 6. Weekly time series of ice thickness and snow depth at Eureka and Alert for (a) low
630 snow years and (b) high snow years.

631

632 Figure 7. Time series of mean air temperature during winter (DJF), spring, (MAM), summer
633 (JJA) and autumn (SON) at the four sites.

634

635 Figure 8. CMIP5 median sea ice thickness seasonal cycle and evolution (1955-2014) at stations
636 (black). Median of ORA-IP models CGLORS, ORAP5.0 and GLORYS2V3 (blue), ECCO-v4
637 (green) and UR025.4 (red). Whiskers indicate the 5th and 95th percentiles.

638

639 Figure 9. Same as Figure 10 for snow depth and only for CMIP5 models.

640

641 Figure 10. Seasonal cycle of observed mean ice thickness (left) and snow depth (right) from
642 PIOMAS at Cambridge Bay and Resolute (1979-2014).

643

644 Figure 11. Comparison of PIOMAS ice thickness with ice thickness observations from
645 Environment Canada's ice thickness monitoring sites at Cambridge Bay and Resolute. The data
646 covers the period 1979-2014.

647

648 Figure 12. **a-e:** Maximum sea ice thickness trends in ORA-IP simulations. **f:** Same for CMIP5
649 MODEL-MEAN. From South to North, o's indicate Cambridge Bay (green), Resolute (blue),
650 Eureka (white) and Alert (black) and x's indicate the corresponding measurement stations. In **f**,
651 one o per model is shown." The stippling indicates p-values less than 0.05, corrected using the
652 False Discovery Rate (FDR) method with a global pFDR-values less than 0.10 [Wilks, 2006].
653 The colorbar is linear from -10 cm dec-1 to 10 cm dec-1 and symmetric logarithmic beyond
654 these values.

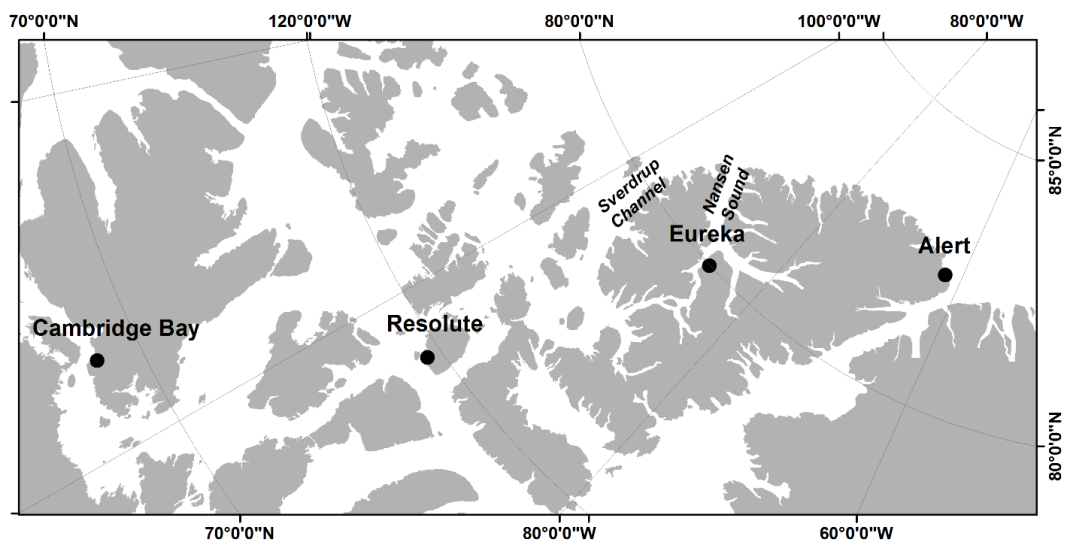
655

656 Figure 13. **a-e:** Pearson correlation of detrended maximum sea ice thickness in ORA-IP with
657 detrended ONDJFMAM ERA-INTERIM 2m temperature. **f:** Same but for CMIP5 MODEL-
658 MEAN. The stippling indicates p-values less than 0.05, corrected using the False Discovery Rate
659 (FDR) method with a global pFDR-values less than 0.10 [Wilks, 2006].

660

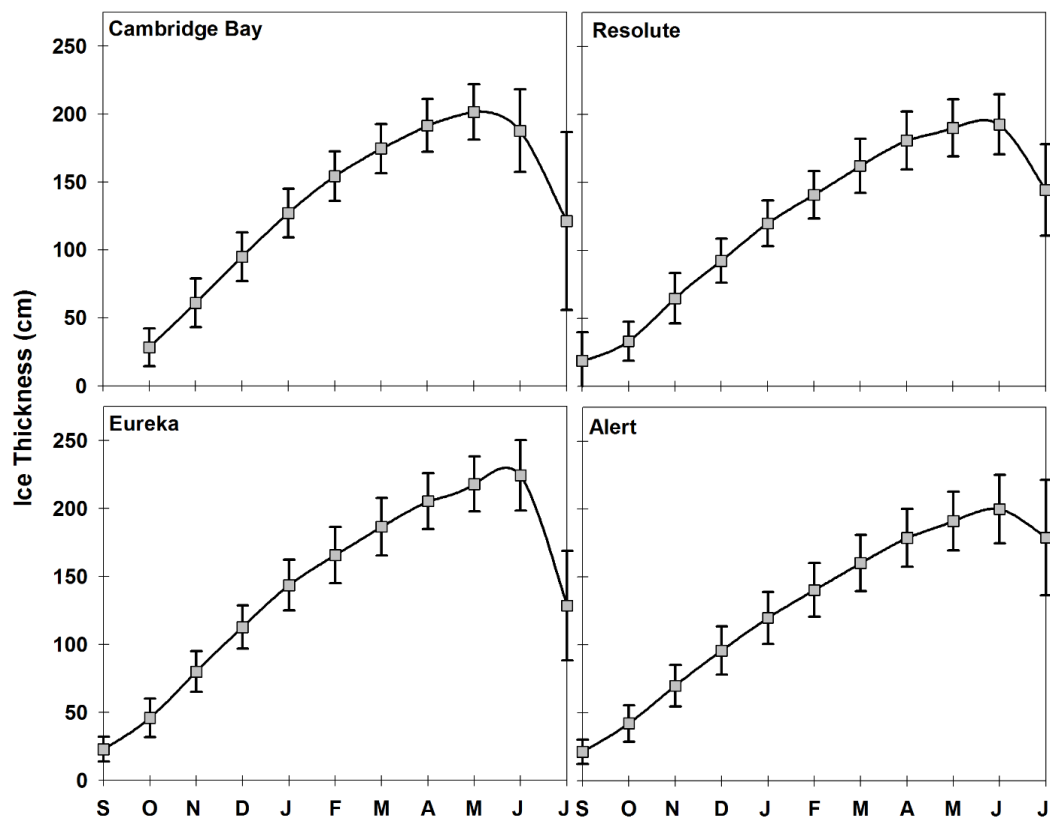


661 Figure 14. Same as Figure 12f but for snow depth trends (ONDFJMAM).
662
663
664
665
666
667
668
669
670
671
672
673
674
675
676
677
678
679
680
681
682
683
684
685
686
687
688
689
690
691
692
693
694
695
696
697
698
699
700



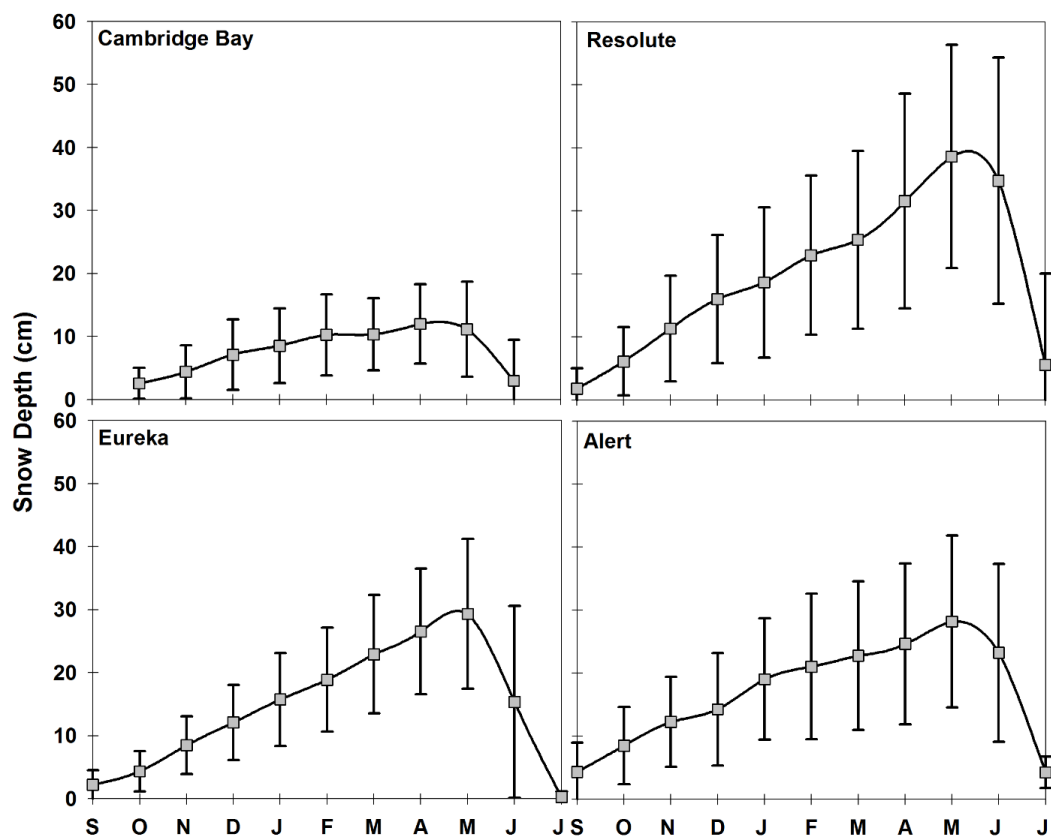
701
702
703
704
705
706
707
708

Figure 1. Map of the central Canadian Arctic Archipelago showing the location of the landfast snow and thickness observations.



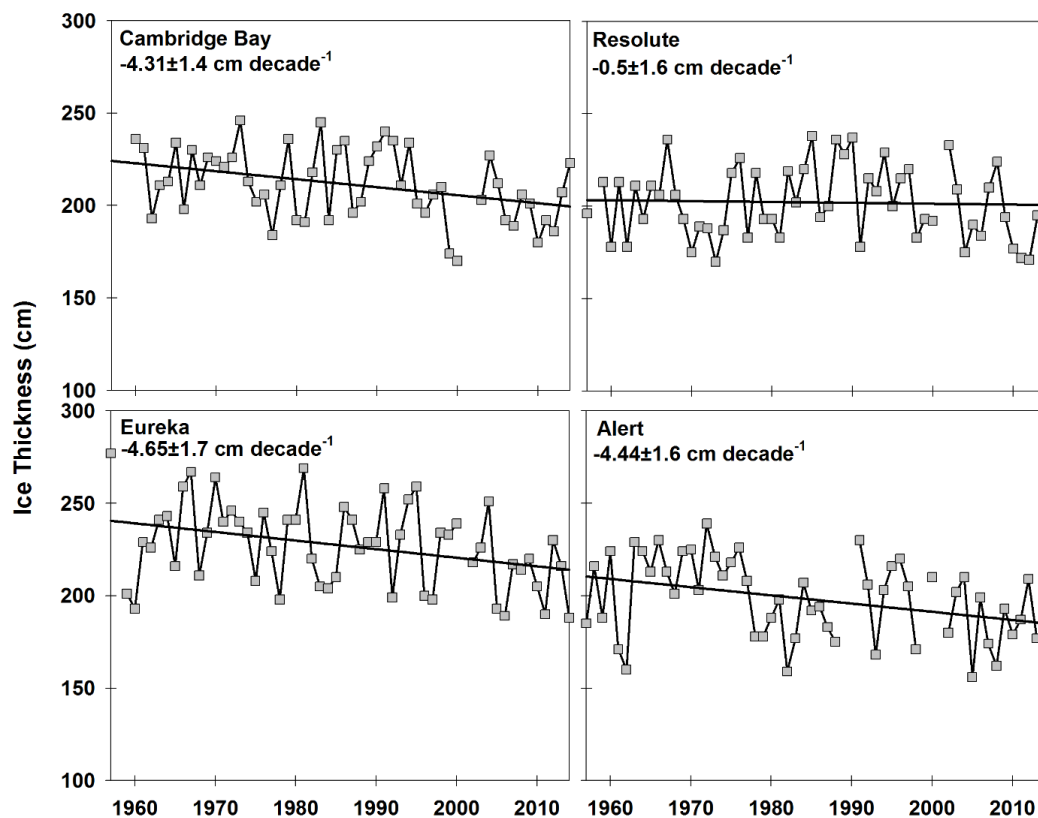
709
710
711
712
713
714
715
716
717
718
719

Figure 2. Seasonal cycle of observed mean ice thickness at the four sites (1960-2014).



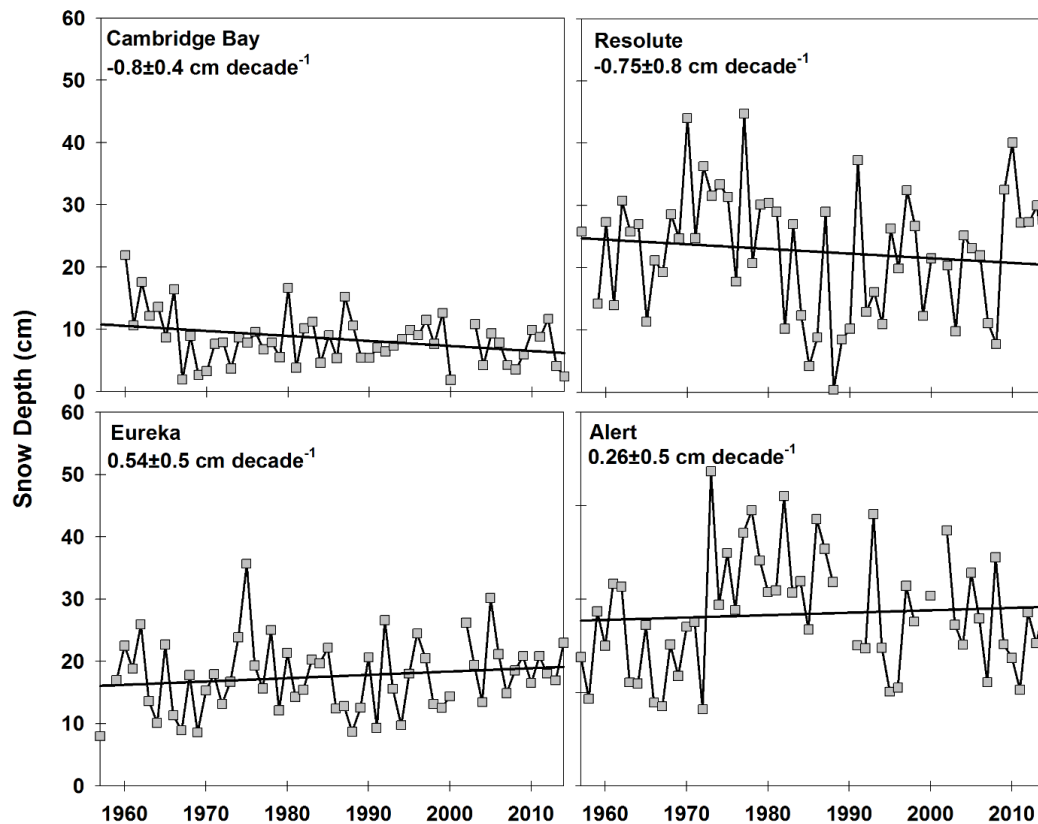
720
721
722
723
724
725
726

Figure 3. Seasonal cycle of observed mean snow depth at the four sites (1960-2014).



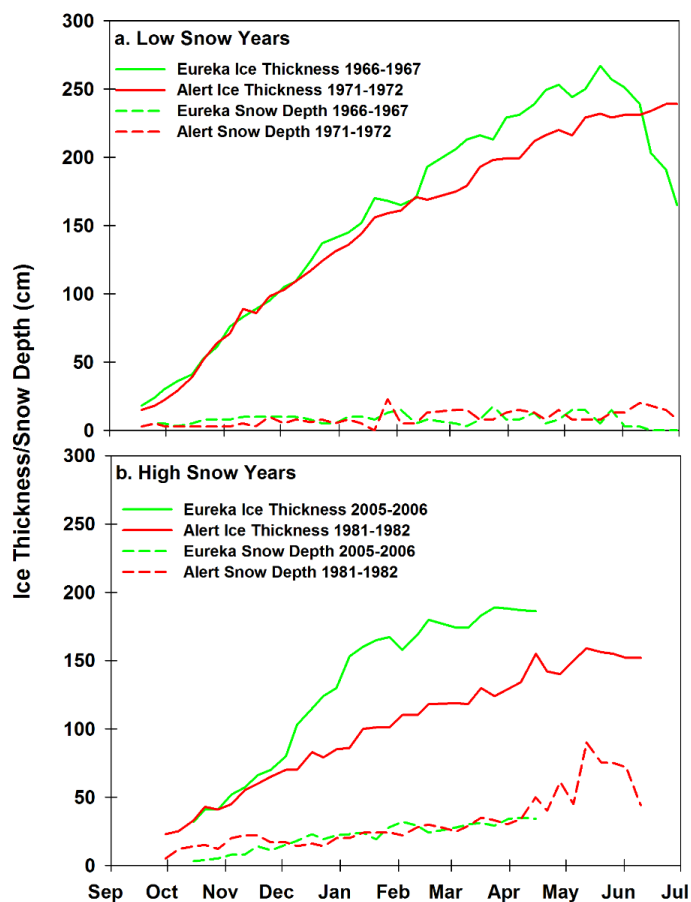
727
728
729
730
731
732
733
734
735
736

Figure 4. Time series and trend of observed maximum ice thickness at the four sites.



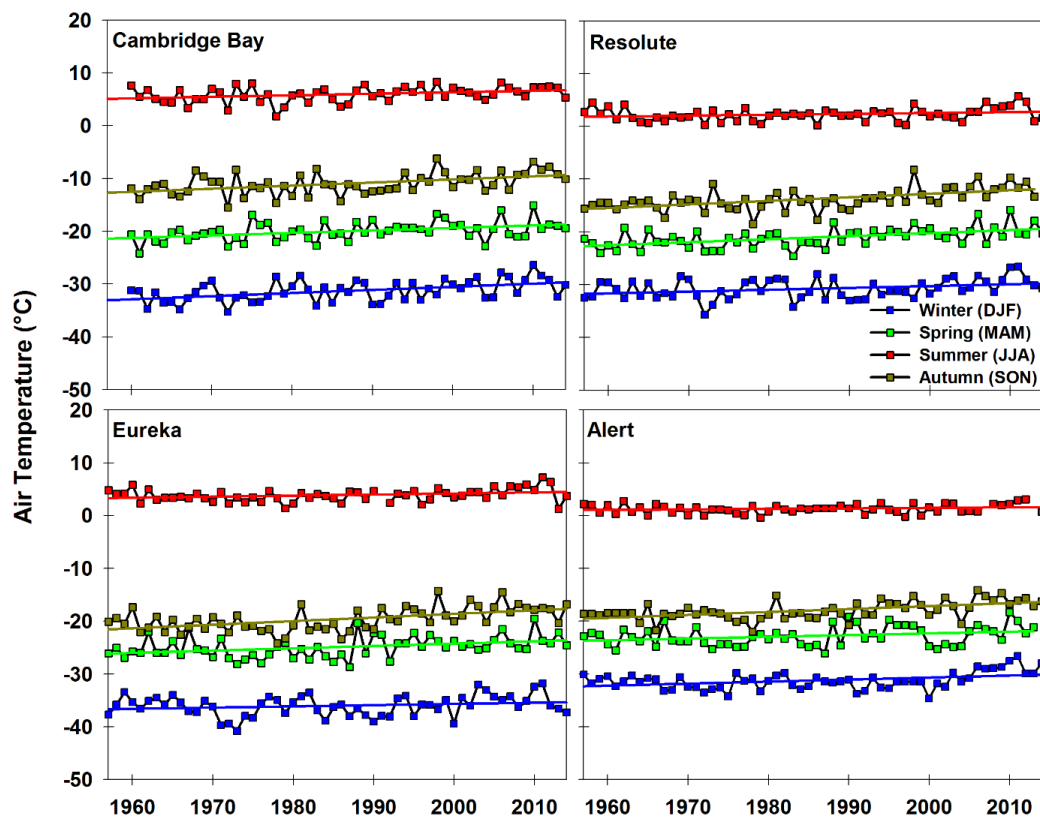
737
738
739
740
741
742
743
744
745

Figure 5. Time series and trend of observed mean October through May snow depth at the four sites.

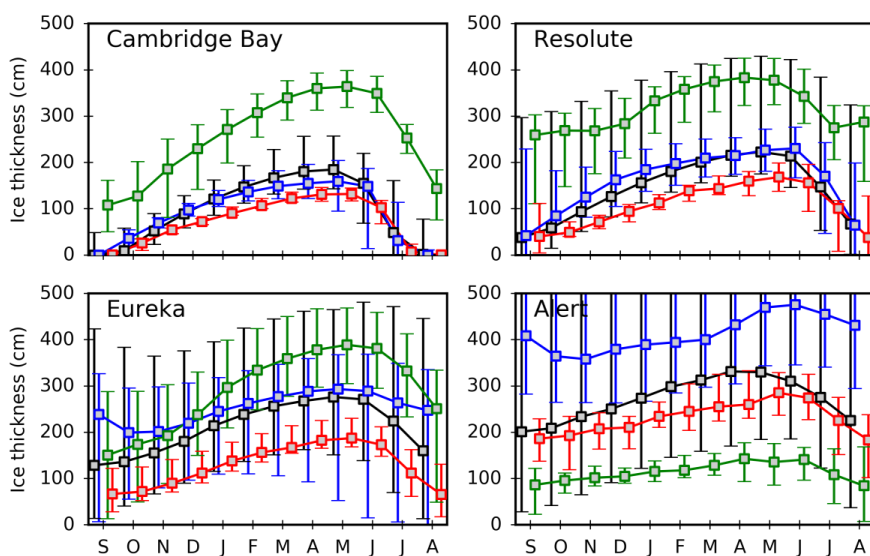


746
747 Figure 6. Weekly time series of ice thickness and snow depth at Eureka and Alert for (a) low
748 snow years and (b) high snow years.
749

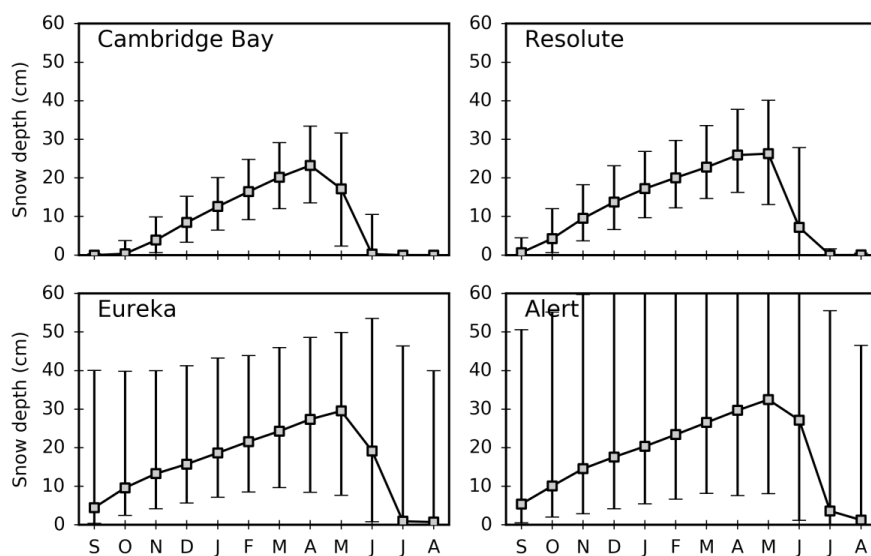
750
751
752



753
754 Figure 7. Time series of mean air temperature during winter (DJF), spring, (MAM), summer
755 (JJA) and autumn (SON) at the four sites.
756
757
758
759

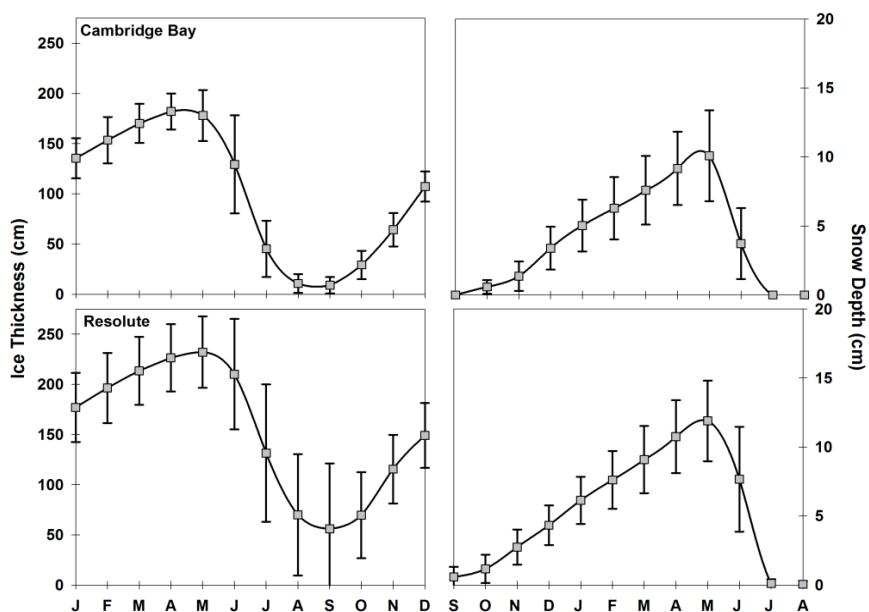


760
761 Figure 8. CMIP5 median sea ice thickness seasonal cycle and evolution (1955-2014) at stations
762 (black). Median of ORA-IP models CGLORS, ORAP5.0 and GLORYS2V3 (blue), ECCO-v4
763 (green) and UR025.4 (red). Whiskers indicate the 5th and 95th percentiles.
764
765
766
767
768
769
770
771



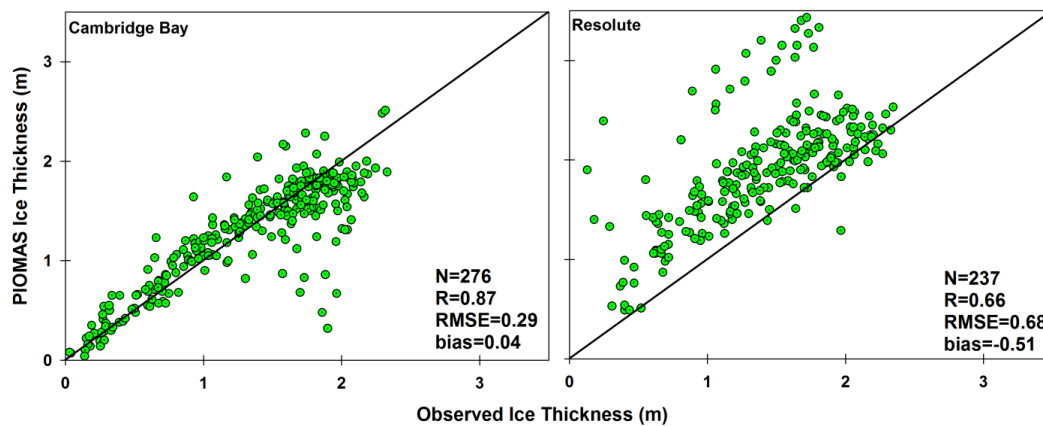
772
773
774
775
776
777
778
779
780
781
782
783
784
785
786
787
788
789
790
791
792
793
794
795
796

Figure 9. Same as Figure 10 for snow depth and only for CMIP5 models.

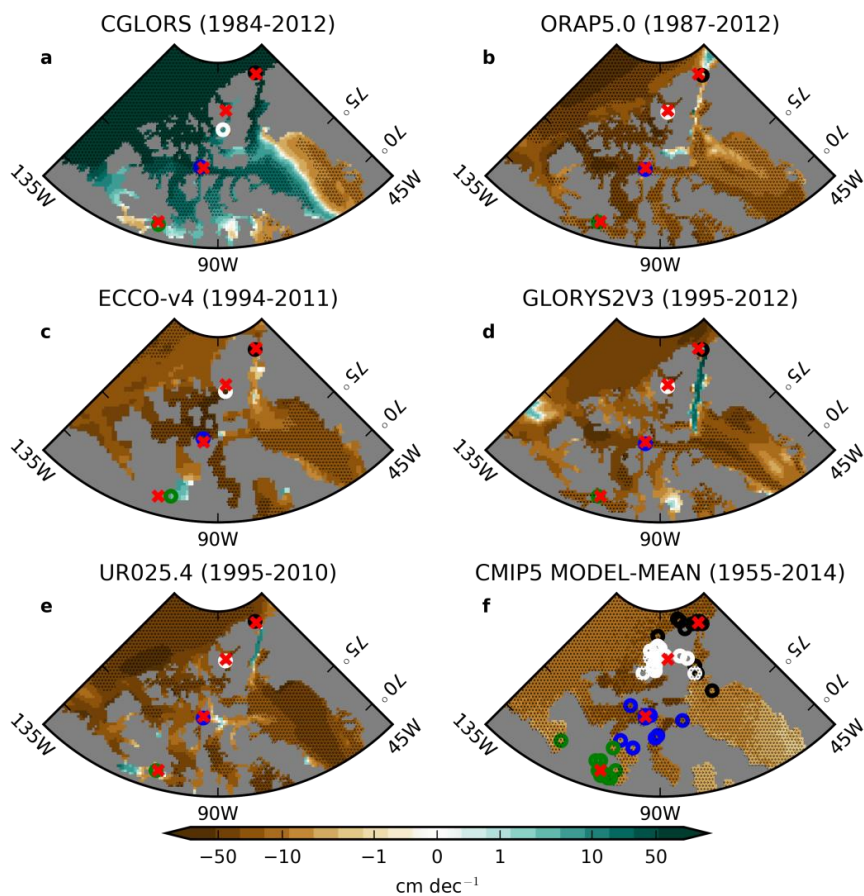


797
798
799
800
801
802
803
804
805
806
807
808
809
810
811
812
813
814
815
816
817
818
819
820
821
822

Figure 10. Seasonal cycle of observed mean ice thickness (left) and snow depth (right) from PIOMAS at Cambridge Bay and Resolute (1979-2014).

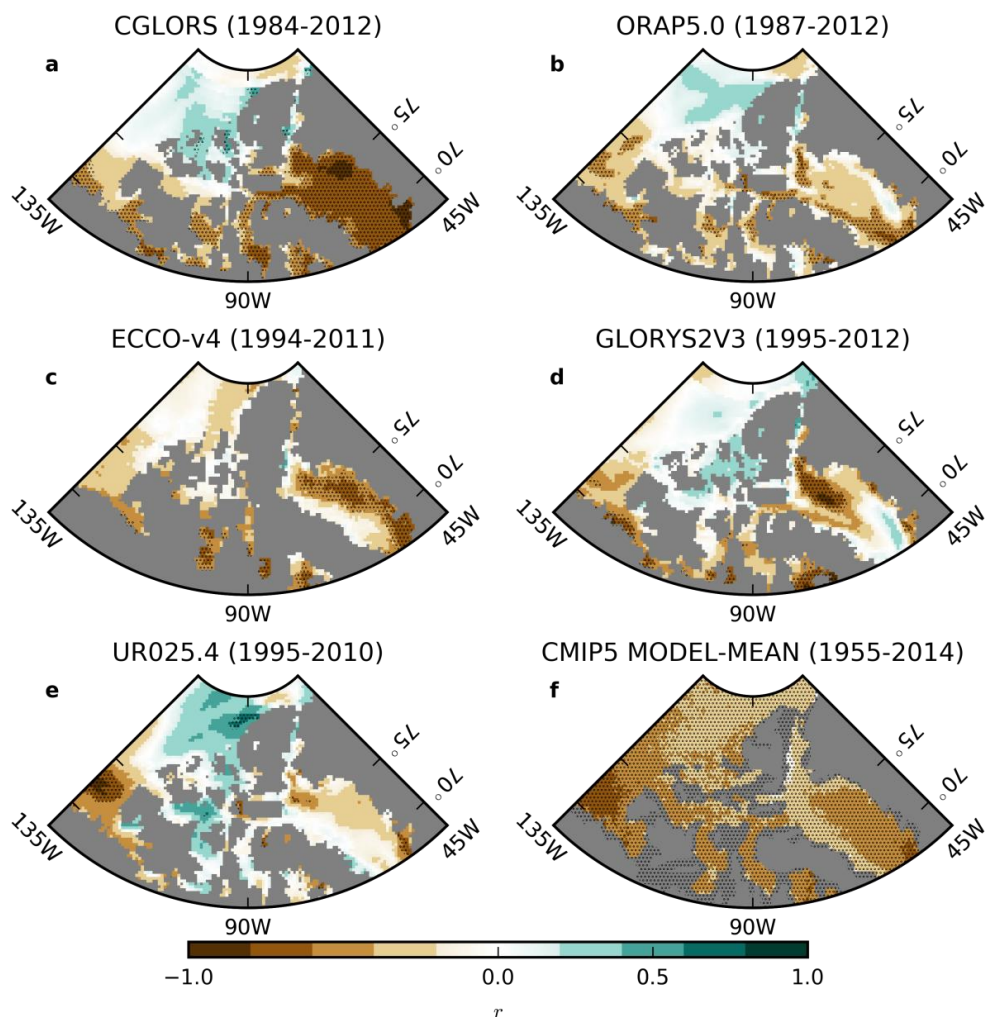


823
824 Figure 11. Comparison of PIOMAS ice thickness with ice thickness observations from
825 Environment Canada's ice thickness monitoring sites at Cambridge Bay and Resolute. The data
826 covers the period 1979-2014.
827
828



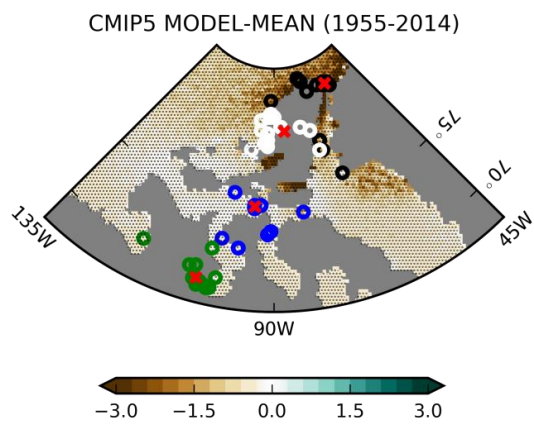
829
 830
 831
 832
 833
 834
 835
 836
 837
 838
 839
 840
 841
 842
 843
 844
 845
 846

Figure 12. **a-e**: Maximum sea ice thickness trends in ORA-IP simulations. **f**: Same for CMIP5 MODEL-MEAN. From South to North, o's indicate Cambridge Bay (green), Resolute (blue), Eureka (white) and Alert (black) and x's indicate the corresponding measurement stations. In f, one o per model is shown." The stippling indicates p-values less than 0.05, corrected using the False Discovery Rate (FDR) method with a global pFDR-values less than 0.10 [Wilks, 2006]. The colorbar is linear from -10 cm dec⁻¹ to 10 cm dec⁻¹ and symmetric logarithmic beyond these values.



847
 848
 849
 850
 851
 852
 853
 854
 855
 856
 857
 858
 859
 860
 861

Figure 13. **a-e**: Pearson correlation of detrended maximum sea ice thickness in ORA-IP with detrended ONDJFMAM ERA-INTERIM 2m temperature. **f**: Same but for CMIP5 MODEL-MEAN. The stippling indicates p-values less than 0.05, corrected using the False Discovery Rate (FDR) method with a global pFDR-values less than 0.10 [Wilks, 2006].



862
863

864 Figure 14. Same as Figure 12f but for snow depth trends (ONDFJMM).